

Dehydrobenzoyl Cations: Distonic Ions with Dual Free Radical and Acylium Ion Reactivity

Luiz Alberto B. Moraes and Marcos N. Eberlin*

Contribution from the Institute of Chemistry, State University of Campinas—UNICAMP,
CP 6154 13083-970 Campinas, SP Brazil

Received April 6, 1998

Abstract: In the gas phase, *m*- and *p*-dehydrobenzoyl cations display strong duality of chemical behavior. The ions react selectively as either free radicals or acylium ions, depending on the choice of the neutral reaction partner. Transacetalization with 2-methyl-1,3-dioxolane, ketalization with 2-methoxyethanol, and epoxide ring expansion with epichlorohydrin demonstrate their acylium ion reactivity, whereas $\cdot\text{SCH}_3$ abstraction with dimethyl disulfide demonstrates their free radical reactivity. In one-pot reactions with gaseous mixtures of epichlorohydrin and dimethyl disulfide, the *m*- and *p*-dehydrobenzoyl cations react selectively at either site to form the two monoderivatized ions in variable but controlled yields; further reaction at either the remaining radical or the acylium charge site forms a single biderivatized ion as the final product. The *o*-dehydrobenzoyl cation also displays the expected radical and acylium ion reactivities. But for the *ortho* isomer, binding of the nucleophilic neutral to the free or derivatized $\text{C}^+=\text{O}$ group facilitates reactions at the radical site. Hence, the *ortho* isomer displays a unique behavior; its acylium ion reactions either occur simultaneously with, or are followed by, H-abstraction radical reactions. As shown by ab initio calculations, the three isomers display σ -localized odd-spin and π -delocalized charge densities, which characterize distonic structures with molecular orbital-separated radical and charge sites. The dehydrobenzoyl cations are also, according to the calculations, the most stable among 19 of the most feasible $\text{C}_7\text{H}_4\text{O}^+$ isomers.

Introduction

Distonic radical cations¹—chemically fascinating ionic species—display two potentially reactive sites: a radical and a positive charge sites formally located, in a conventional valence bond description, at different atoms or group of atoms. Because of this unique, unconventional electronic structure, the chemical behavior of distonic ions may be driven by either the radical or the positive charge site, or by both. Most reactions so far reported for distonic ions are, however, of the radical type, the charge site playing a subsidiary role.^{2,3}

Distonic radical cations with chemically reactive free radicals and chemically inert charge sites have been tested as models⁴ for, and have shown properties⁵ of, charged radicals. In such species, the charge site serves just as a “handle” for mass

spectrometric manipulation. Phenyl radicals with coordinatively saturated charged substituents have been shown to be best models for charged radicals,⁴ allowing investigations in the gas-phase MS environment of the intrinsic chemical behavior of free radicals. Effective separation of the radical and charge sites by the rigid phenyl ring prevents the neutral reagent from binding—and eventually reacting—at the charge site; hence, the ions display typical radical reactions.⁴

While distonic ions with coordinatively saturated and chemically inert charge sites allow one to explore separately free radical reactivity, even more chemically attractive distonic ions would provide access to both free radical and ion reactivity in a single molecule. For a distonic ion to provide this dual, noninterfering chemical behavior, the ion must bear formally separated and reactive radical and charge sites; a rigid spacer such as the phenyl ring or other locked molecular framework would also be required.

Sound candidates for distonic ions with such dual chemical behavior are charged phenyl radicals with coordinatively unsaturated, thus potentially reactive, charged substituents. Acylium ions, important reactive carbocations in the condensed phase,⁶ are stable, easily accessible, and of rich and characteristic reactivity^{7–11} in the gas phase. Considering, therefore, both the

(1) (a) Yates, B. F.; Bouma, W. J.; Radom, L. *J. Am. Chem. Soc.* **1984**, *106*, 5805. (b) Radom, L.; Bouma, W. J.; Nobes, R. H. *Pure Appl. Chem.* **1984**, *56*, 1831. (c) Yates, B. F.; Bouma, W. J.; Radom, L. *Tetrahedron* **1986**, *42*, 6225.

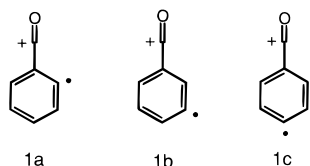
(2) (a) Hammerum, S. *Mass Spectrom. Rev.* **1988**, *7*, 123. (b) Bouchoux, G. *Mass Spectrom. Rev.* **1988**, *7*, 203. (c) Stirk, K. M.; Kiminkinen, M. L. K.; Kenttämää, H. I. *Chem. Rev.* **1992**, *92*, 1649.

(3) (a) Bouma, W. J.; MacLeod, J. K.; Radom, L. *Adv. Mass Spectrom.* **1980**, *8A*, 178. (b) Miller, D. L.; Gross, M. L. *Org. Mass Spectrom.* **1983**, *18*, 239. (c) Stirk, K. G.; Kenttämää, H. I. *J. Am. Chem. Soc.* **1991**, *113*, 5880. (d) Rusli, R. D.; Schwarz, H. *Chem. Ber.* **1990**, *123*, 535. (e) Mourgues, P.; Audier, H. E.; Leblanc, D.; Hammerum, S. *Org. Mass Spectrom.* **1993**, *28*, 1098. (f) van Amsterdam, M. W.; Staneke, P. O.; Ingemann, S.; Nibbering, N. M. M. *Org. Mass Spectrom.* **1993**, *28*, 919. (g) Smith, R. L.; Chyall, L. J.; Stirk, K. M.; Kenttämää, H. I. *Org. Mass Spectrom.* **1993**, *28*, 1623. (h) de Koster, C. G.; van Houte, J. J.; van Thuijl, J. *Int. J. Mass Spectrom. Ion Processes* **1995**, *141*, 1. (i) Gozzo, F. C.; Eberlin, M. N. *J. Am. Soc. Mass Spectrom.* **1995**, *6*, 554. (j) Li, R.; Schweighofer, A.; Keck, H.; Kuchen, W.; Kenttämää, H. I. *Int. J. Mass Spectrom. Ion Processes* **1996**, *157/158*, 293. (k) Eberlin, M. N.; Sorriha, A. E. P. M.; Gozzo, F. C.; Pimpim, R. S. *J. Am. Chem. Soc.* **1997**, *119*, 3550.

(4) (a) Stirk, K. M.; Smith, R. L.; Orłowski, J. C.; Kenttämää, H. I. *Rapid Commun. Mass Spectrom.* **1993**, *7*, 392. (b) Chyall, L. J.; Kenttämää, H. I. *J. Am. Chem. Soc.* **1994**, *116*, 3135. (c) Smith, R. L.; Kenttämää, H. I. *J. Am. Chem. Soc.* **1995**, *117*, 1393. (d) Thoen, K. K.; Smith, R. L.; Nousiainen, J. J.; Nelson, E. D.; Kenttämää, H. I. *J. Am. Chem. Soc.* **1996**, *118*, 8669.

(5) (a) Flammang, R.; Thoelen, O.; Quattrocchi, C.; Bredas, J.-L. *Rapid Commun. Mass Spectrom.* **1992**, *6*, 135. (b) Yu, S. J.; Holliman, C. L.; Rempel, D. L.; Gross, M. L. *J. Am. Chem. Soc.* **1993**, *115*, 9676. (c) Sorriha, A. E. P. M.; Gozzo, F. C.; Pimpim, R. S.; Eberlin, M. N. *J. Am. Soc. Mass Spectrom.* **1996**, *7*, 1126.

characteristic chemistry of gaseous acylium ions and the interest in distonic ions with dual free radical and ion chemical reactivities, isomeric dehydrobenzoyl cations (**1a,c**), in which the radical and acylium charge sites are formally located in "electronically isolated" σ - and π -molecular orbitals, are attractive candidates.



Novel gas-phase reactions have been proposed as general methods for the characterization of both distonic radical^{12,13} and acylium ions.^{9–11} Driven by their highly odd-spin populated radical sites, distonic ions abstract $\cdot\text{SCH}_3$ from dimethyl disulfide¹² and $\cdot\text{SeCH}_3$ from dimethyl diselenide.¹³ Likewise, acylium ions react generally with cyclic acetals and ketals by transacetalization,⁹ by direct ketalization with diols and analogues,¹⁰ and by ring expansion with epoxides.¹¹

We report here a study aimed at investigating whether gaseous *o*-, *m*-, and *p*-dehydrobenzoyl cations **1a–c** display the expected dual chemical behavior. Free radical reactivity was tested via $\cdot\text{SCH}_3$ abstractions with dimethyl disulfide, and acylium ion reactivity via three characteristic reactions: transacetalization with 2-methyl-1,3-dioxolane, ketalization with 2-methoxyethanol, and epoxide ring expansion with epichlorohydrin. Ab initio calculations predict the electronic structures and relative stabilities of the ions of interest, and are used to compare them with other $\text{C}_7\text{H}_4\text{O}^{+\bullet}$ isomers.

Methods

The gaseous ions were produced, reacted, and their products analyzed via double- (MS^2) and triple-stage (MS^3) mass spectrometric experiments¹⁴ performed with an Extrel (Pittsburgh, PA) pentaquadrupole

(6) Olah, G. A.; Gramain, A.; White, A. M. In *Carbonium Ions*; Olah, G. A., Schleyer, P. v. R., Eds.; Wiley: New York, 1976; Vol. 5, Chapter 35.

(7) (a) Chatfield, D. A.; Bursey, M. M. *J. Am. Chem. Soc.* **1976**, *98*, 6492. (b) Staley, R. H.; Wieting, R. D.; Beauchamp, J. L. *J. Am. Chem. Soc.* **1977**, *99*, 5964. (c) Sparapani, C.; Speranza, M. *J. Am. Chem. Soc.* **1980**, *102*, 3120. (d) Kim, J. K.; Caserio, M. C. *J. Am. Chem. Soc.* **1982**, *104*, 4624. (e) Attinà, M.; Cacace, F. *J. Am. Chem. Soc.* **1983**, *105*, 1122. (f) Paradisi, C.; Kenttämäa, H. I.; Le, Q. T.; Caserio, M. C. *Org. Mass Spectrom.* **1988**, *23*, 521. (g) Kotiaho, T.; Eberlin, M. N.; Shay, B. J.; Cooks, R. G. *J. Am. Chem. Soc.* **1993**, *115*, 1004. (h) Creaser, C. S.; Williamson, B. L. *J. Chem. Soc., Perkin Trans. 2* **1996**, 427.

(8) (a) Eberlin, M. N.; Majumdar, T. K.; Cooks, R. G. *J. Am. Chem. Soc.* **1992**, *114*, 2884. (b) Eberlin, M. N.; Cooks, R. G. *J. Am. Chem. Soc.* **1993**, *115*, 9226.

(9) (a) Eberlin, M. N.; Cooks, R. G. *Org. Mass Spectrom.* **1993**, *28*, 679. (b) Gozzo, F. C.; Sorrihla, A. E. P. M.; Eberlin, M. N. *J. Chem. Soc., Perkin Trans. 2* **1996**, 587. (c) Moraes, L. A. B.; Gozzo, F. C.; Eberlin, M. N.; Vainiotalo, P. *J. Org. Chem.* **1997**, *62*, 5096. (d) Moraes, L. A. B.; Eberlin, M. N. *J. Chem. Soc., Perkin Trans. 2* **1997**, 2105. (e) Carvalho, M. C.; Moraes, L. A. B.; Kascheres, C.; Eberlin, M. N. *J. Mass Spectrom.* **1997**, *32*, 1137. (f) Carvalho, M. C.; Juliano, V. F.; Kascheres, C.; Eberlin, M. N. *J. Chem. Soc., Perkin Trans. 2* **1997**, 2347. (g) Carvalho, M.; Gozzo, F. C.; Mendes, M. A.; Sparrapan, R.; Kascheres, C.; Eberlin, M. N. *Chem. Eur. J.* **1998**, *4*, 1161.

(10) (a) Moraes, L. A. B.; Pimpim, R. S.; Eberlin, M. N. *J. Org. Chem.* **1996**, *61*, 8726. (b) Augusti, R.; Gozzo, F. C.; Moraes, L. A. B.; Sparrapan, R.; Eberlin, M. N. *J. Org. Chem.* **1998**, *63*, 4889.

(11) Moraes, L. A. B.; Eberlin, M. N. *J. Org. Chem.* Submitted for publication.

(12) Stirk, K. M.; Orłowski, J. C.; Leeck, D. T.; Kenttämäa, H. I. *J. Am. Chem. Soc.* **1992**, *114*, 8604.

(13) Beasley, B. J.; Smith, R.; Henttämäa, H. I. *J. Mass Spectrom.* **1995**, *30*, 384.

(14) Eberlin, M. N. *Mass Spectrom. Rev.* **1997**, *16*, 113.

mass spectrometer.¹⁵ The instrument, denoted $\text{Q}_1\text{q}_2\text{Q}_3\text{q}_4\text{Q}_5$, is composed of a sequential arrangement of three mass-analyzing (Q_1 , Q_3 , Q_5) and two "rf-only" ion-focusing reaction quadrupoles (q_2 , q_4). The reactant ions were formed by 70-eV electron ionization (EI) of either 2'-, 3'-, or 4'-nitroacetophenone or phthalic anhydride. In the MS^2 ion/molecule reactions, Q_1 was used to mass-select the ion of interest. The neutral reagent was then added to q_2 , and reactions occurred at translational energies near 0 eV, as calculated from the m/z 39:41 ratio in neutral ethylene/ionized ethylene reactions.¹⁶ Product ion spectra were acquired by scanning Q_5 , while operating Q_3 in the broad band rf-only mode. The target gas pressures in q_2 caused typical beam attenuations of 50–70%, viz., multiple collision conditions were used, which increases reaction yields while promoting collisional quenching of both the reactant and product ions.¹⁴ Lower reaction yields but similar sets of ionic products were also observed at lower pressure, single-collision conditions in q_2 .

For the MS^3 experiments,¹⁷ Q_3 was used to mass-select the product ion of interest for further 15-eV collision dissociation with argon in q_4 , while scanning Q_5 to record the spectrum. The 15-eV collision energy was calculated as the voltage difference between the ion source and the collision quadrupoles. The indicated pressures in each differentially pumped region were typically 2×10^{-6} (ion-source), 8×10^{-6} (q_2), and 8×10^{-5} (q_4) Torr, respectively.

Ab initio molecular orbital calculations were run on Gaussian94.¹⁸ The geometries of **1a–c** were fully optimized at the ROHF/6-311+G(d,p) level of theory,¹⁹ whereas improved energies were obtained by single-point calculations at the ROMP2²⁰/6-311+G(2df,2p)//ROHF/6-311+G(d,p) level. ROMP2/6-311G(d,p)//ROHF/6-31G(d,p) calculations provided the relative energies of the $\text{C}_7\text{H}_4\text{O}^{+\bullet}$ isomers **1–17**.

Results and Discussion

Dissociation Behavior. The isomeric 2'-, 3'-, and 4'-nitroacetophenones were first selected as potential precursors of the dehydrobenzoyl cations **1a–c**. Dissociative 70-eV EI of the nitroacetophenones would produce **1a–c** if dissociations follow the direct cleavages summarized in Scheme 1.

Scheme 1

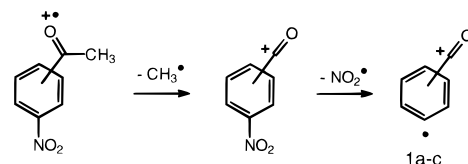


Figure 1 compares the low-energy (15 eV) MS^2 collision-induced dissociation (CID) spectra of the m/z 104 ions isolated after ionization of the isomeric nitroacetophenones. The ions thought to be **1b** (Figure 1b) and **1c** (Figure 1c) lose consecutively neutral molecules of 28 (m/z 76) and 26 u (m/z 50), i.e., most likely CO and C_2H_2 . As rationalized for **1c** in Scheme 2, the dehydrobenzoyl cation structures **1b** and **1c** account satisfactorily for such dissociation behavior.

(15) Juliano, V. F.; Gozzo, F. C.; Eberlin, M. N.; Kascheres, C.; Lago, C. L. *Anal. Chem.* **1996**, *68*, 1328.

(16) Tiernan, T. O.; Futrell, J. H. *J. Phys. Chem.* **1968**, *72*, 3080.

(17) Schwartz, J. C.; Wade, A. P.; Enke, C. G.; Cooks, R. G. *Anal. Chem.* **1990**, *62*, 1809.

(18) Frisch, M. J.; Trucks, G. W.; Schlegel, H. B.; Gill, P. M. W.; Johnson, B. G.; Robb, M. A.; Cheeseman, J. R.; Keith, T.; Petersson, G. A.; Montgomery, J. A.; Raghavachari, K.; Al-Laham, M. A.; Zakrzewski, V. G.; Ortiz, J. V.; Foresman, J. B.; Peng, C. Y.; Ayala, P. Y.; Chen, W.; Wong, M. W.; Andres, J. L.; Replogle, E. S.; Gomperts, R.; Martin, R. L.; Fox, D. J.; Binkley, J. S.; Defrees, D. J.; Baker, J.; Stewart, J. P.; Head-Gordon, M.; Gonzalez, C.; Pople, J. A. *GAUSSIAN94*, Revision B.3; Gaussian, Inc.: Pittsburgh, PA, 1995.

(19) Frisch, M. J.; Pople, J. A.; Binkley, J. S. *J. Chem. Phys.* **1984**, *80*, 3265.

(20) Møller, C.; Plesset, M. S. *Phys. Rev.* **1934**, *46*, 618.

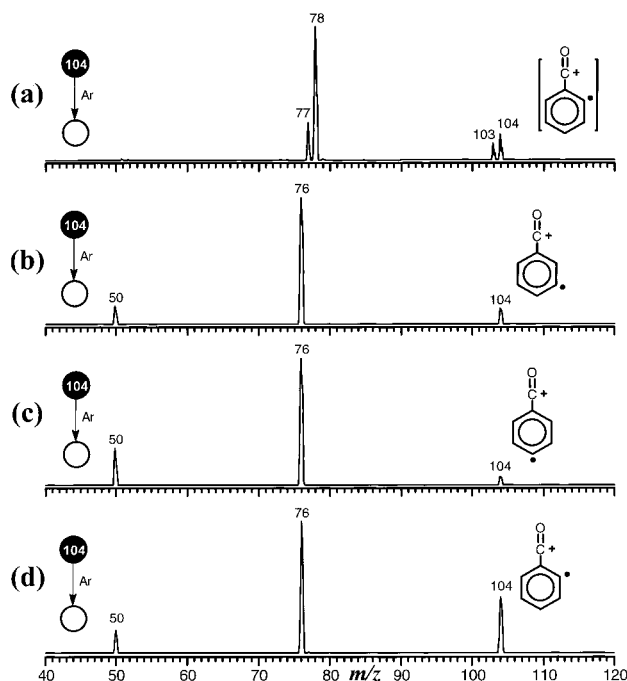
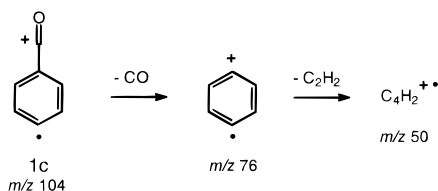
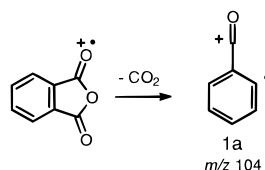


Figure 1. Double-stage (MS^2) 15-eV CID product spectra of the m/z 104 70-eV EI fragment ions of (a) 2-nitro-, (b) 3-nitro-, and (c) 4-nitroacetophenone and (d) phthalic anhydride. Note in spectra b–d identical dissociation behaviors that characterize the dehydrobenzoyl cations, and in spectrum a the contrasting dissociation behavior that suggests an isomeric structure. In the terminology used to describe MS^2 experiments and scan modes, a filled circle represents a fixed (or selected) mass and an open circle a variable (or scanned) mass, whereas the neutral reagent or collision gas that causes the mass transitions are shown between the circles. For more details on this terminology, see ref 17.

Scheme 2



Scheme 3



The ion thought to be **1a** (Figure 1a) displays, however, distinctive CID behavior; it dissociates apparently by two competitive sequences: H loss (m/z 103) followed by C_2H_2 loss (m/z 77), and C_2H_2 loss (m/z 78) followed by H loss (m/z 77). These findings allow two interpretations: that an isomeric $C_7H_4O^{+\bullet}$ ion, not **1a**, is formed from 2'-nitroacetophenone, or that the dissociation behavior of **1a** is greatly influenced by an *ortho* effect.

Phthalic anhydride is also a potential precursor of **1a** (Scheme 3). The CID spectrum of the m/z 104 ion isolated after ionization of phthalic anhydride was also recorded (Figure 1d). The ion displays dissociation behavior nearly identical to those of **1b** (Figure 1c) and **1c** (Figure 1d), which suggests formation

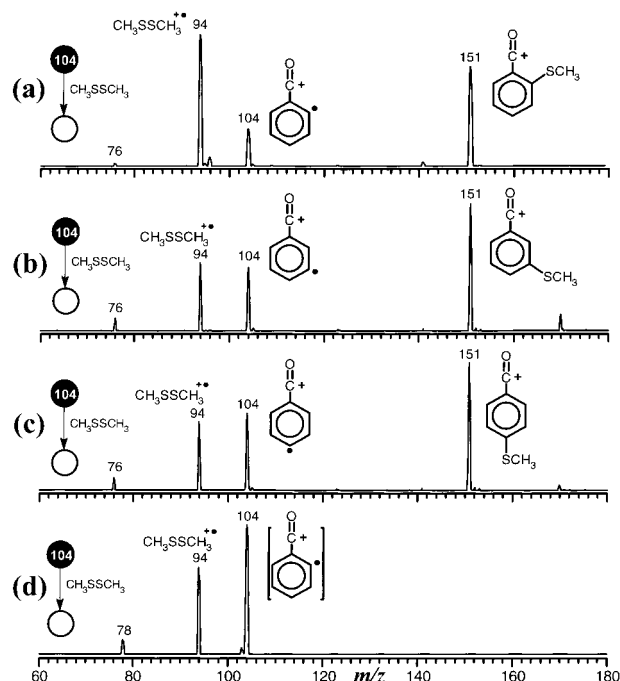


Figure 2. Double-stage (MS^2) product spectra for reaction with dimethyl disulfide of the putative ions (a) **1a**, (b) **1b**, (c) **1c**, and (d) an isomeric $C_4H_7O^{+\bullet}$ ion. Note in spectra a–c the major $\bullet SCH_3$ abstraction product of m/z 151, and in spectrum a the dominance of the charge-transfer product of m/z 94.

of **1a**. This finding suggests also that 2'-nitroacetophenone forms not **1a** but an isomeric $C_7H_4O^{+\bullet}$ (Figure 1a).

Free Radical Reactivity: $\bullet SCH_3$ Abstraction. Figure 2 compares the double-stage (MS^2) product ion spectra for **1a**–**1c**/dimethyl disulfide reactions. The *tandem-in-space* mode of operation of the QqQq Q^{15} permitted reaction conditions to be kept unchanged when reacting each of the three isomers. The free radical reactivities of **1a** (Figure 2a), **1b** (Figure 2b), and **1c** (Figure 1c) with CH_3SSCH_3 are evident, as they all abstract $\bullet SCH_3$ to form the m/z 151 product ion (Scheme 4, pathway a). The isomeric (and unknown) $C_4H_7O^{+\bullet}$ ion derived from 2'-nitroacetophenone does not display free radical reactivity with dimethyl disulfide; it reacts predominantly by charge transfer to yield $CH_3SSCH_3^{+\bullet}$ of m/z 94 (Figure 2d). This chemical behavior provides evidence against a distonic ion structure.¹²

$CH_3SSCH_3^{+\bullet}$ of m/z 94 is also formed in **1a**–**1c**/dimethyl disulfide reactions. It was noted, however, that the use of slightly higher collision energies increases the relative abundances of both the m/z 76 fragment ion and $CH_3SSCH_3^{+\bullet}$ (m/z 94), while decreasing correspondingly that of the m/z 151 $\bullet SCH_3$ abstraction product. Further, reactions with dimethyl disulfide of the m/z 76 fragment ions sampled directly from the ion source form $CH_3SSCH_3^{+\bullet}$ to a great extent (data not shown). These findings suggest charge transfer from the **1a**–**1c** fragment ion of m/z 76 to be an important pathway to $CH_3SSCH_3^{+\bullet}$.

Acylium Ion Reactivity: (i) Transacetalization. Figure 3a–c compares the MS^2 product ion spectra for **1a**–**1c**/2-methyl-1,3-dioxolane reactions. Characteristic acylium ion behavior for **1b** and **1c** is evident as they react promptly via transacetalization⁹ to afford the cyclic ionic ketals of m/z 148 (Scheme 4, pathway b). Formal hydride (m/z 87) and methyl anion abstractions (m/z 73) yield the two other reaction products. CO loss (m/z 76), which probably displays a relatively low dissociation threshold, also occurs in minor to moderate extents (Figure 3). Although very low collision energies (near 1 eV) are applied for the ion/molecule reactions, dissociation may still

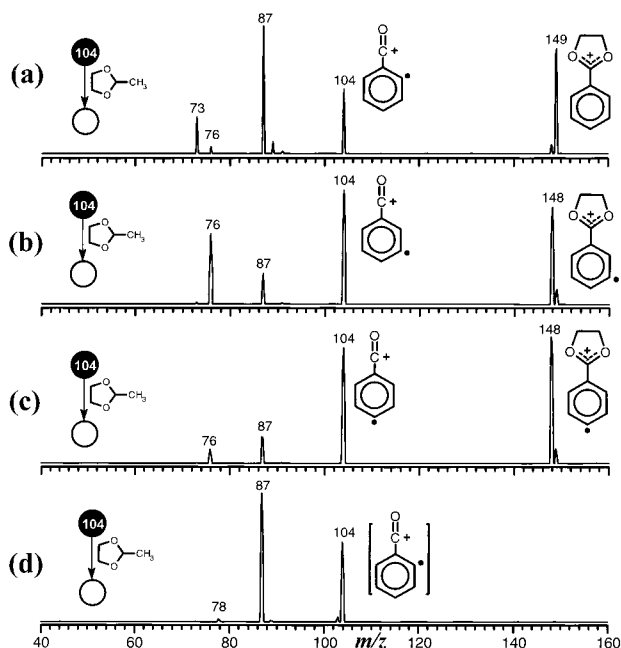
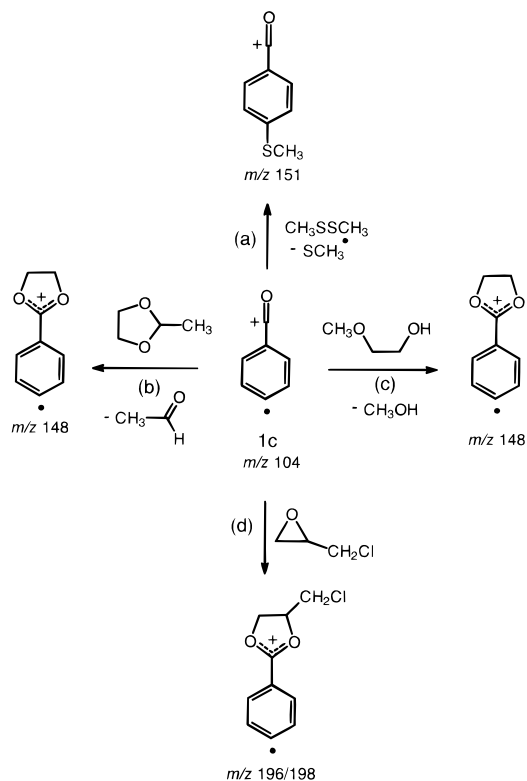


Figure 3. Double-stage (MS^2) product spectra for reactions with 2-methyl-1,3-dioxolane of (a) **1a**, (b) **1b**, (c) **1c**, and (d) an isomeric $C_4H_7O^+$ ion. Note the transacetalization/H-abstraction product of m/z 149 in spectrum a, the transacetalization product of m/z 148 in spectra b and c, and the dominance of the formal hydride abstraction product of m/z 87 in spectrum d. In spectra a–c, the m/z 76 ion corresponds to CO loss from the reactant ions.

Scheme 4



occur, owing to the initial internal energy of the ions and the high efficiency of translational to internal energy transfer in quadrupole collision cells.²¹

The *ortho* isomer **1a** is, however, unique; it reacts with 2-methyl-1,3-dioxolane to yield the m/z 149 product (Figure

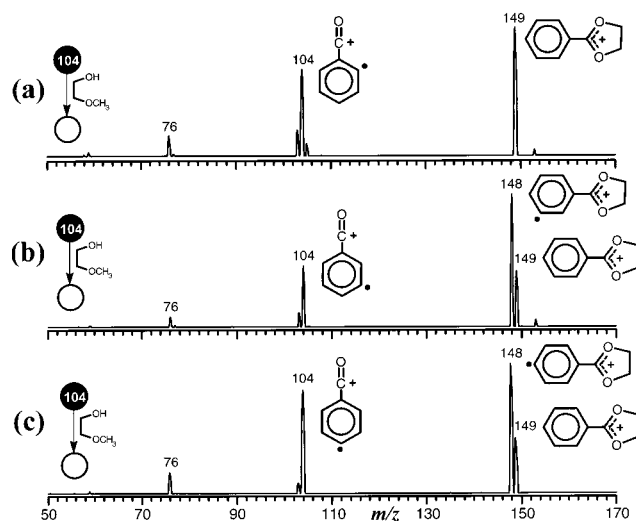
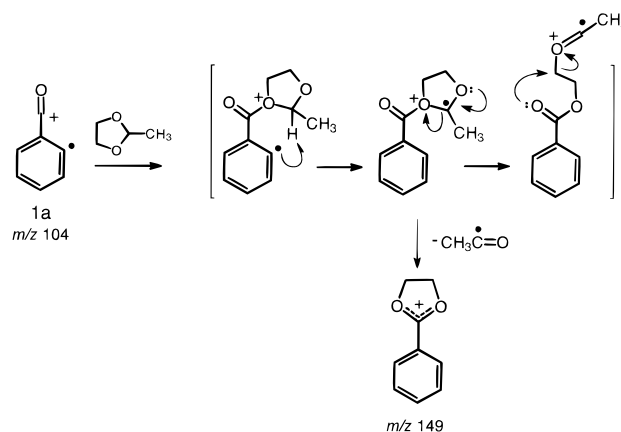


Figure 4. Double-stage (MS^2) product spectra for reactions with methoxyethanol of (a) **1a**, (b) **1b**, and (c) **1c**. Note in spectrum a the dominance of the ketalization/H-abstraction product of m/z 149 and in spectra b and c formation of both m/z 149 and the ketalization product of m/z 148.

Scheme 5



3a), apparently via simultaneous transacetalization/H-abstraction. As the use of lower pressures of 2-methyl-1,3-dioxolane was unsuccessful in detecting any m/z 148 reaction intermediate, the simultaneous transacetalization/H-abstraction mechanism depicted in Scheme 5 is suggested for direct formation of m/z 149 from **1a**. Note that binding of the nucleophilic 2-methyl-1,3-dioxolane to the $C^+=O$ group facilitates H-abstraction by the *ortho* radical site.

Again, the isomeric $C_4H_7O^+$ ion from 2'-nitroacetophenone displays no transacetalization reactivity (Figure 3d), chemical behavior that eliminates an acylium ion structure.⁹

(ii) Ketalization. Figure 4 compares the product ion spectra for **1a**–**c**/2-methoxyethanol reactions. Ketalization⁹ (Scheme 3, pathway c) yields the m/z 148 product and occurs promptly for **1b** (Figure 4b) and **1c** (Figure 4c), but a m/z 149 product ion is also formed. In the m/z 148 ketalization product (Scheme 3, pathway c), the radical site remains active; hence, the ions further abstract H from 2-methoxyethanol to yield the corresponding closed shell ion of m/z 149, i.e., the benzoyl cation protected in the ketal form. When lower pressures of 2-methoxyethanol are used, the relative abundance of m/z 149 decreases sharply. As no direct H-abstraction product of m/z 105 is formed, **1b** and **1c** must display ketalization reactivities with 2-methoxyethanol which are greater than their H-abstraction reactivities.

(21) Douglas, D. J. *J. Am. Soc. Mass Spectrom.* **1998**, *9*, 101.

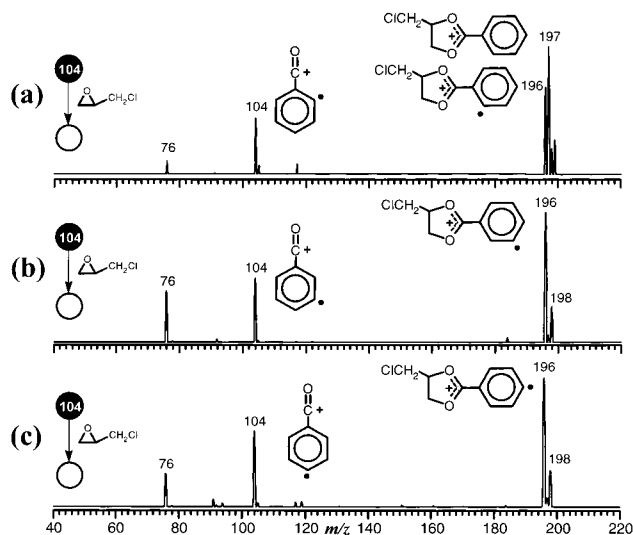
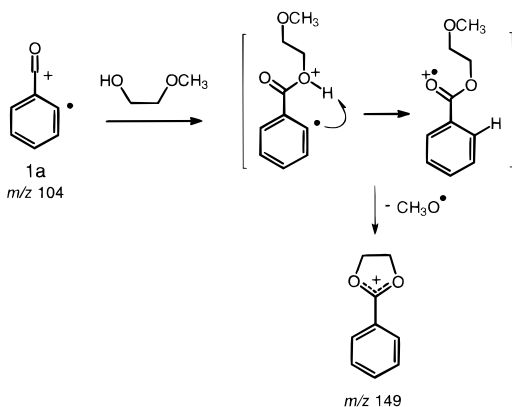


Figure 5. Double-stage (MS^2) product spectra for reactions with epichlorohydrin of (a) **1a**, (b) **1b**, and (c) **1c**. Note in spectra b and c the epoxide ring expansion product of m/z 196/198 and in spectrum a the formation of both m/z 196/198 and the epoxide ring expansion/H-abstraction product of m/z 197/199.

Scheme 6



The *ortho* isomer **1a** is again unique; it forms directly the m/z 149 product (Figure 4a). The ketalization product of m/z 148 was not detected, even when using considerably lower pressures of 2-methoxyethanol; hence, simultaneous ketalization/H-abstraction facilitated by initial binding to $C^+=O$ and the *ortho* position of the radical site is proposed (Scheme 6).

(iii) Epoxide Ring Expansion. Figure 5 compares the product ion spectra for **1a–c**/epichlorohydrin reactions. Epoxide ring expansion (Scheme 3, pathway d) occurs for the three isomers, forming the product ion of m/z 196/198 (Figure 5). The *ortho* isomer **1a** (Figure 5c) displays again unique behavior; its epoxide ring expansion products react further by H-abstraction to form the chlorine isotopomers of m/z 197/199. As the single H-abstraction product of m/z 105 is also observed, two alternative reaction sequences are equally likely: H-abstraction followed by epoxide ring expansion, or epoxide ring expansion followed by H-abstraction. Lower pressures of epichlorohydrin relatively favor both the m/z 105 and 196/198 products. That only the *ortho* isomer **1a** (and its epoxide ring expansion product) reacts by H-abstraction is rationalized by the neighboring location of the acylium charge and radical site. Binding of epichlorohydrin to the free or derivatized $C^+=O$ group or formation of loosely $C^+=O$ bonded ion/neutral complexes (the solvated ion) would favor H-abstraction by the *ortho* radical site. These findings further demonstrate the

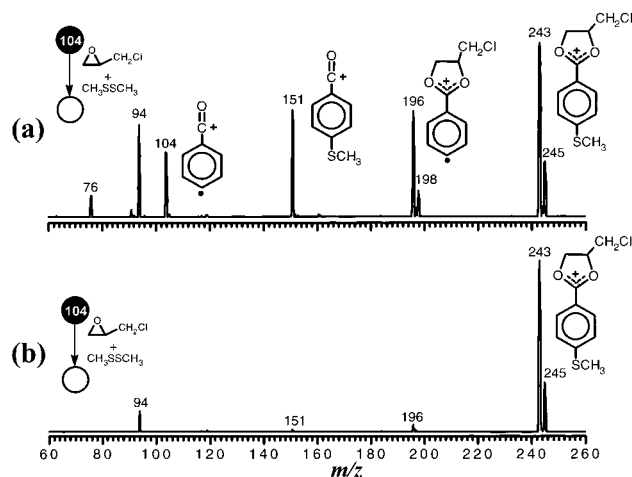
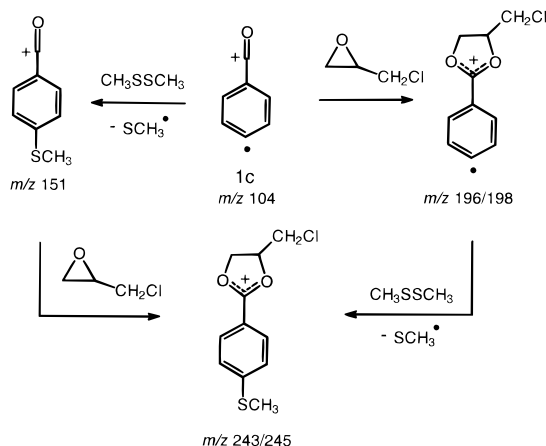


Figure 6. Double-stage (MS^2) product spectra for reaction of **1c** with a gaseous mixture of neutral epichlorohydrin and dimethyl disulfide performed at (a) lower and (b) higher q_2 pressures. Nearly identical spectra were obtained in reactions of **1b**. Note in spectrum a the two intermediate monoderivatized products of m/z 151 and 196/198, and the final biderivatized product of m/z 243/245, whereas in spectrum b the higher q_2 pressures, and hence the greater number of reactive collisions, favor formation of the final biderivatized product of m/z 243/245.

Scheme 7



pronounced acylium ion reactivity of **1a–c**, and the unique proclivity of **1a** to undergo both acylium and radical (H-abstraction) reactions in either a simultaneous or a stepwise fashion.

Duality of Chemical Behavior. To test the ions' ability to react selectively at either the radical or charge site, and then react further at the remaining reactive site, one-pot reactions of **1b,c** with gaseous mixtures of dimethyl disulfide and epichlorohydrin were performed. Figure 6 exemplifies the spectrum of **1c**, which is nearly identical to that of **1b** (not shown).

One-pot reactions (Figure 6a) form the three expected products: the two monoderivatized ions of m/z 151 and 196/198 and the biderivatized ion of m/z 243/245 (Scheme 7). The $C^+=O$ group in the epoxide ring expansion product of m/z 196/198 is now chemically saturated (protected as a cyclic ionic ketal),^{9,10} but the radical site remains chemically reactive; hence, the ion further abstracts $\cdot SCH_3$ from dimethyl disulfide to yield the biderivatized product of m/z 243/245. Similarly, primary radical reactions with dimethyl disulfide yield the $\cdot SCH_3$ abstraction product, i.e., the even-electron acylium ion of m/z 151, which reacts further by epoxide ring expansion with

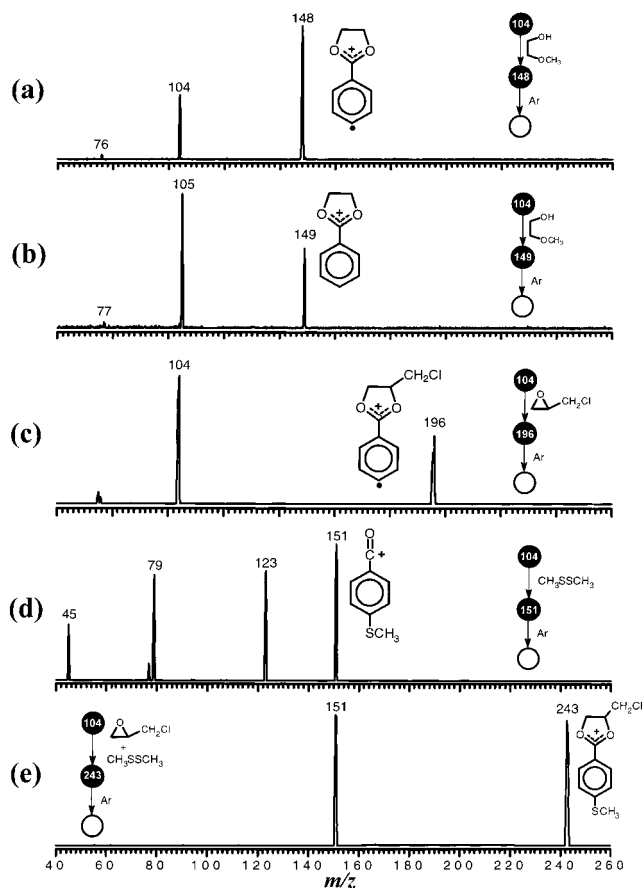


Figure 7. Triple-stage (MS^3) sequential product spectra for the product ions of (a) transacetalization, (b) transacetalization plus H-abstraction, (c) epoxide ring expansion, (d) $\cdot S\text{CH}_3$ abstraction, and (e) epoxide ring expansion plus $\cdot S\text{CH}_3$ abstraction of **1c**. Nearly identical spectra were obtained for the product ions of **1b**. Note that all four cyclic ionic ketals, i.e., both the closed-shell and the open-shell dioxolanylium ions, dissociate, re-forming the reactant acylium ion; the $\cdot S\text{CH}_3$ abstraction product loses consecutively CO and CS.

epichlorohydrin at the free acylium charge site, $\text{C}^+=\text{O}$, to form the same biderivatized product of m/z 243/245 (Scheme 7).

Yields of the one-pot reaction are easily controlled. When varying the pressures, i.e., the relative concentration of each neutral reagent in the q2 gaseous mixture, the abundance ratio of the two intermediates of m/z 151 and 196/198 changes correspondingly; the sequential reactions proceed practically to completion under higher neutral reagent pressures (Figure 6b). Near complete ion conversion to the m/z 243/245 biderivatized product suggests that, by far, the majority of the reactant ion population is composed of **1b** or **1c**. As already mentioned, the minor product ion of m/z 94 ($\text{CH}_3\text{SSCH}_3^+$) likely results from charge transfer with the m/z 76 fragment ion.

Structural Characterization. The product ion structures were examined via triple-stage (MS^3) CID experiments. Figure 7 collects the most representative spectra. All the cyclic ionic ketals (Figure 7a–c,e), both the odd- and even-electron ones, display the expected, characteristic dissociation behavior; they re-form exclusively the reactant acylium ion (Scheme 8).^{9–11} Just as condensed-phase hydrolysis of neutral acetals and ketals frees the protected aldehydes or ketones,²² so gas-phase CID of the ionic ketals frees the protected acylium ions.

The $\cdot S\text{CH}_3$ abstraction product of m/z 151 (Figure 7d) displays a richer and characteristic dissociation behavior. As expected

Scheme 8

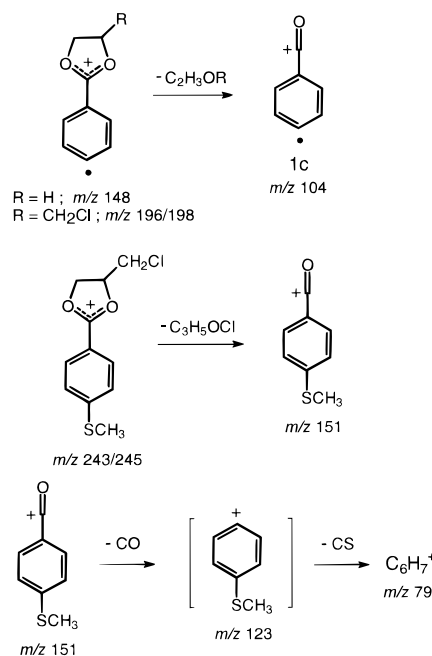


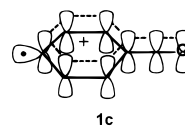
Table 1. Total and Relative Energies of the Dehydrobenzoyl Cations from *ab Initio* Calculations

species	ROHF/6-311+G(d,p) (hartrees)	ROMP2/6-311+G(2df,2p)// ROHF/6-311+G(d,p) (hartrees)	relative energy (kcal/mol)
1a	−342.01479	−343.27747	2.0
1b	−342.01412	−342.27900	1.0
1c	−342.01734	−343.28060	zero

for a benzoyl cation derivative,⁸ it loses CO to form the m/z 123 fragment, whereas apparently further CH_3 shift isomerization followed by CS loss forms the m/z 79 fragment (Scheme 8).

Ab Initio Calculations. (i) Charge and Odd-Spin Densities. The dehydrobenzoyl cations' electronic energies and charge and odd-spin densities, and those of the benzoyl cation and the phenyl radical, were estimated by ROMP2/6-311+G-(2df,2p)//ROHF/6-311+(d,p) *ab initio* MO calculations. Energy differences within **1a–c** are found to be very small (Table 1), increasing by only 2.0 kcal/mol when moving from the most stable (**1c**) to the least stable dehydrobenzoyl cation isomer (**1a**).

Charge and odd-spin densities of **1a–c** parallel those of the benzoyl cation and the phenyl radical (Figure 7), respectively; hence, the three isomeric dehydrobenzoyl cations display electronic structures characteristic of both σ -localized phenyl radicals and π -delocalized aromatic benzoyl cations. From such electronic structures and by using the usual conventional valence bond description,^{1,2} **1a–c** are not properly classified as distonic ions with *spatially* separated radical and spin sites. Applying, however, molecular orbital formalism, the σ -localized radical sites and π -delocalized charge sites of **1a–c** (see representation below for **1c**) characterize distonic ions not with spatially separated, but with *molecular orbital*-separated radical and spin sites.



Although for the three isomers the radical-bearing carbons display nearly identical spin densities (0.80–0.82 e), their

(22) Kunz, H. In *Comprehensive Organic Synthesis*; Trost, B. M., Fleming, I., Eds.; Pergamon Press: New York, 1991; Vol. 59, p 659.

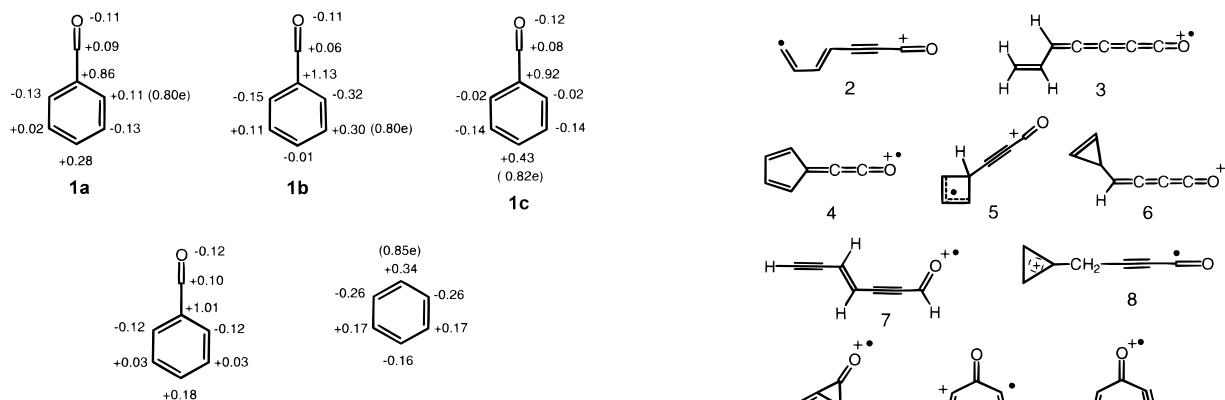


Figure 8. Ab initio ROMP2/6-311+G(2df,2p)//6-311+G(d,p) Mulliken charge and odd-spin distributions of the dehydrobenzoyl cations **1a–c** and of the benzoyl cation and the phenyl radical. For simplicity, the values for the hydrogen atoms were summed into the carbon atoms.

Table 2. Total and Relative Energies of $C_7H_4O^+$ Isomers from ab Initio Calculations

species ^a	ROHF/6-31G(d,p) (hartrees)	ROMP2/6-311G(d,p)// ROHF/6-31G(d,p) (hartrees)	relative energy (kcal/mol)
1a	−341.94552	−343.09340	zero
1b	−341.94465	−343.09458	0.8
1c	−341.94796	−343.09606	1.7
2	−341.84097	−342.99268	63.2
3	−341.85306	−343.01537	49.0
4	−341.88632	−343.03775	34.9
5	−341.82687	−342.99921	59.1
6	−341.81062	−342.99049	64.6
7	−341.80731	−342.93383	100.1
8	−341.80774	−342.96121	82.9
9	−341.88725	−343.01488	49.3
11	−341.84657	−342.99567	61.3
12	−341.82455	−342.97235	76.0
13	−341.80172	−342.95045	89.7
14	−341.87975	−343.03415	37.2
15	−341.92951	−343.00650	54.5
16	−341.82182	−342.95865	84.6
17	−341.82479	−342.95792	85.0

^a Ion **10** is unstable; it ring-closes to **9** without any appreciable energy barrier during geometry optimization.

positive charges differ significantly (Figure 8): **1a**, +0.11; **1b**, +0.30; and **1c**, +0.43. Higher electron deficiency at the radical site of distonic ions has been shown to favor radical reactions,^{4,23} and this effect apparently induces the higher relative yields of the \cdot SCH₃ abstraction products of *m/z* 151 (Figure 2).

(ii) $C_7H_4O^+$ Isomers. If one considers that the nascent *m/z* 104 ion from 2'-nitroacetophenone (first thought to be **1a**) is inherently unstable and isomerizes rapidly, there would be no difficulty in accounting for its contrasting dissociation and chemical behavior, as the ion may lose its dual acylium ion and free radical reactivity as the result of isomerization. Further, a possible instability of such an ion raises also the question of whether **1a–c** isomerize to more stable $C_7H_4O^+$ isomers, ones which could also display distonic structures with dual chemical behavior. Trying to answer these questions, the energies of **1a–c** and 16 additional conventional and distonic $C_7H_4O^+$ isomers (**2–17**) were evaluated via ROMP2/6-311G(d,p)//ROHF/6-31G(d,p) ab initio calculations.

Most $C_7H_4O^+$ isomers, except **10** which ring-closes to **9** during geometry optimization, are found to be stable by the calculations (Table 2). The dehydrobenzoyl cations **1a–c** are,

however, by far the most stable isomers; hence, their isomerizations to **2–17** are thermodynamically unfavorable in the gas phase. Isomerizations among **1a–c** by H ring-walking²⁴ are predicted to be nearly endothermic (within theoretical errors); hence, they cannot be excluded. However, H-walking in pyridyl cation rings has been shown by high-accuracy CBS-Q ab initio calculations to be kinetically hampered by barriers as high as 75 kcal/mol;²⁵ further, the observed unique chemistry of **1a** proves that it does not easily interconvert to **1b** or **1c**.

Conclusion

Dehydrobenzoyl cations, the most stable $C_7H_4O^+$ isomers, are distonic ions with molecular orbital-separated σ -localized radical and π -delocalized acylium charge sites. Owing to this unique electronic structure, and the chemically unsaturated, reactive acylium charge site, the *meta* and *para* isomers display strong duality of chemical behavior in the gas phase; they react selectively either as free radical or acylium ions. They behave, depending on the choice of the neutral reaction partner, either as free radicals with an inert charge site or as even-electron acylium ions with an inert radical site.

The dual chemical behavior of the *m*- and *p*-dehydrobenzoyl cations is best demonstrated by one-pot reactions with two selected neutrals. With dimethyl disulfide and epichlorohydrin, the ions first react at either their radical or acylium charge sites to form two monoderivatized intermediates; further reaction at the remaining radical or acylium charge site forms a single, biderivatized ion as the final product.

The *ortho*-dehydrobenzoyl cation also displays a similar σ -localized radical and π -delocalized cation structure and the expected radical and acylium ion reactivities. But for the *ortho* isomer, binding of nucleophilic neutrals at the free or derivatized $C^+=O$ group facilitates reactions at the neighboring *ortho* radical site, which confers to the ion a unique behavior; its acylium

(23) Avila, D. V.; Ingold, K. U.; Luszyk, J.; Dolbier, W. R., Jr.; Pan, H.-Q.; Muir, M. *J. Am. Chem. Soc.* **1994**, *116*, 99.

(24) Gallup, G. A.; Steinheider, D.; Gross M. L. *Int. J. Mass Spectrom. Ion Phys.* **1976**, *22*, 185.

(25) Gozzo, F. C.; Mendes, M. A.; Carvalho, M.; Sparrapan, R.; Eberlin, M. N. *J. Org. Chem.* In press.

ion reactions either occur simultaneously with, or are followed by, H-abstraction radical reactions.

Acknowledgment. Financial support by the Research Support Foundation of the State of São Paulo (FAPESP) and the Brazilian National Research Council (CNPq) is greatly ac-

knowledged. This paper is dedicated to Prof. J. M. Riveros in recognition of his inspiring, incisive, and continuous contribution to gas-phase ion chemistry.

JA981152L